



Shrunk halo and quenched shell gap at $N = 16$ in ^{22}C : Inversion of sd states and deformation effects

Xiang-Xiang Sun^{a,b}, Jie Zhao^c, Shan-Gui Zhou^{a,b,d,e,*}^a CAS Key Laboratory of Theoretical Physics, Institute of Theoretical Physics, Chinese Academy of Sciences, Beijing 100190, China^b School of Physical Sciences, University of Chinese Academy of Sciences, Beijing 100049, China^c Microsystem and Terahertz Research Center, China Academy of Engineering Physics, Chengdu 610200, Sichuan, China^d Center of Theoretical Nuclear Physics, National Laboratory of Heavy Ion Accelerator, Lanzhou, 730000, China^e Synergetic Innovation Center for Quantum Effects and Application, Hunan Normal University, Changsha, 410081, China

ARTICLE INFO

Article history:

Received 11 August 2018

Received in revised form 28 August 2018

Accepted 29 August 2018

Available online 3 September 2018

Editor: W. Haxton

Keywords:

 ^{22}C

Shrunk halo

 $(2s_{1/2}, 1d_{5/2})$ inversion

Shape decoupling

Deformed RHB model in continuum

ABSTRACT

We explore the interplays among the formation of a halo, deformation effects, the inversion of sd states, the shell evolution, and changes of nuclear magicities in ^{22}C by using a deformed relativistic Hartree–Bogoliubov model in continuum. It is revealed that there is an inversion between the two spherical orbitals $2s_{1/2}$ and $1d_{5/2}$ in ^{22}C compared with the conventional single particle shell structure in stable nuclei. This inversion, together with deformation effects, results in a shrunk halo and a quenched shell gap at $N = 16$. It is predicted that the core of ^{22}C is oblate but the halo is prolate. Therefore several exotic nuclear phenomena, including the halo, the shape decoupling effects, the inversion of sd states, and the evolution of shell structure which results in (dis)appearance of magic numbers, coexist in one single nucleus ^{22}C .

© 2018 The Author(s). Published by Elsevier B.V. This is an open access article under the CC BY license (<http://creativecommons.org/licenses/by/4.0/>). Funded by SCOAP³.

1. Introduction

The study of exotic nuclear structure is at the forefront of research in modern nuclear physics [1]. Among many others, the most striking exotic nuclear phenomenon is the nuclear halo which was first observed in ^{11}Li [2]. Halo nuclei are weakly bound and well associated with pairing correlations and the contribution of the continuum above the threshold of particle emission [3–12]. The formation of a nuclear halo is closely connected with the evolution of the shell structure and changes of nuclear magicities around drip-lines [13–16].

Most known nuclei are deformed with shapes deviating from a sphere. When the deformation is involved in, even more exotic phenomena are expected [17]. The shape decoupling phenomenon, i.e., the core and the halo having different shapes, has been predicted in deformed nuclei close to the neutron drip-line [18,19]. For example, in $^{42,44}\text{Mg}$, the core and the halo are predicted to be prolate and oblate, respectively. Such predictions were made by using a deformed relativistic Hartree–Bogoliubov model in con-

tinuum (DRHBC model) [18–20] which describes self-consistently the large spatial extension, the contribution of the continuum due to pairing correlations, and deformation effects in deformed nuclei with halos. Later similar shape decoupling effects were also revealed by using nonrelativistic Skyrme Hartree–Fock–Bogoliubov models for axially deformed nuclei in coordinate space [21–24] or in a Gaussian basis [25,26].

As the heaviest Borromean nucleus with a halo observed so far, ^{22}C is of particular interest because of not only possible new magicities but also uncertainties and puzzles in the separation energy, the matter radius, and the halo configuration. If the $Z = 6$ magic number evidenced in neutron-rich C isotopes [27] persists in it and the shell gap at $N = 16$ is large enough, ^{22}C could be a new doubly magic nucleus [28]. The empirical value of the two-neutron separation energy S_{2n} is 420(940) keV in AME2003 [29] and 110(60) keV in AME2012 [30–32]. In 2012, S_{2n} was determined to be -0.14 ± 0.46 MeV from direct mass measurements [33]. According to the recent AME2016, $S_{2n} = 35(20)$ keV [34–36]. The matter radius of ^{22}C deduced from interaction cross sections measured in two experiments differ very much: $r_m = 5.4 \pm 0.9$ fm in 2010 [37] and $r_m = 3.44 \pm 0.08$ fm in 2016 [38]. Recently, the determination of ^{22}C radius with interaction cross sections was re-examined by using the Glauber model and $r_m = 3.38 \pm 0.10$ fm was

* Corresponding author at: CAS Key Laboratory of Theoretical Physics, Institute of Theoretical Physics, Chinese Academy of Sciences, Beijing 100190, China.

E-mail address: sgzhou@itp.ac.cn (S.-G. Zhou).

extracted [39]. In almost all investigations on ^{22}C [37–61], the two valence neutrons are assumed to occupy mostly the second s orbital $2s_{1/2}$. There are strong interplays among S_{2n} , r_m , and the halo configuration, see, e.g., Ref. [62] for a recent review. An apparent puzzle arises from these interplays: if the two valence neutrons occupy $2s_{1/2}$ and S_{2n} is very small, say, from several tens keV to several hundreds keV, the radius of ^{22}C should be much larger than the recent experimental value.

In this work, we study ^{22}C with the DRHBC model. It is shown that the $2s_{1/2}$ orbital is a bit lower than the $1d_{5/2}$ orbital when the spherical symmetry is imposed, i.e., these two states are inverted compared with the conventional shell structure in stable nuclei. The near degeneracy of $2s_{1/2}$ and $1d_{5/2}$ would lead to a large shell gap at $N = 16$. However, the ground state of ^{22}C is deformed. The inversion of $(2s_{1/2}, 1d_{5/2})$, together with deformation effects, results in a shrinkage in the halo and a quenched shell gap at $N = 16$ in ^{22}C , thus resolving the puzzles concerning the radius and halo configuration in this exotic nucleus. Furthermore, we predict that the core of ^{22}C is oblate but the halo is prolate, adding one more candidate of deformed halo nuclei with shape decoupling effects.

2. The DRHBC model

The details of the DRHBC model with nonlinear meson-nucleon couplings can be found in Refs. [18–20]. The DRHBC model with density-dependent couplings has been developed by Chen et al. [63]. Here we only present briefly the formalism for the convenience of the following discussions. In the DRHBC model, the RHB equation for nucleons [64]

$$\begin{pmatrix} h_D - \lambda & \Delta \\ -\Delta^* & -h_D^* + \lambda \end{pmatrix} \begin{pmatrix} U_k \\ V_k \end{pmatrix} = E_k \begin{pmatrix} U_k \\ V_k \end{pmatrix}, \quad (1)$$

is solved in a Woods-Saxon (WS) basis [65] which can describe the large spatial extension of halo nuclei. In Eq. (1), h_D is the Dirac Hamiltonian, λ is the chemical potential, and E_k and $(U_k, V_k)^T$ are the quasiparticle energy and wave function. The pairing potential reads,

$$\Delta(\mathbf{r}_1, \mathbf{r}_2) = V^{pp}(\mathbf{r}_1, \mathbf{r}_2)\kappa(\mathbf{r}_1, \mathbf{r}_2), \quad (2)$$

with a density dependent force of zero-range

$$V^{pp}(\mathbf{r}_1, \mathbf{r}_2) = V_0 \delta(\mathbf{r}_1 - \mathbf{r}_2) \left(1 - \frac{\rho(\mathbf{r}_1)}{\rho_{\text{sat}}}\right) \frac{1}{2}(1 - P^\sigma), \quad (3)$$

and the pairing tensor $\kappa(\mathbf{r}_1, \mathbf{r}_2)$ [66,67]. In the Dirac Hamiltonian [68–76]

$$h_D = \boldsymbol{\alpha} \cdot \mathbf{p} + V(\mathbf{r}) + \beta(M + S(\mathbf{r})), \quad (4)$$

the scalar and vector potentials are expanded in terms of the Legendre polynomials,

$$f(\mathbf{r}) = \sum_\lambda f_\lambda(r) P_\lambda(\cos \theta), \quad \lambda = 0, 2, 4, \dots, \quad (5)$$

so are various densities in the DRHBC model. Note that for tri-axially deformed nuclei, the expansion of potentials and densities should be made in terms of spherical harmonics [77].

Our calculations are carried out with the covariant density functional PK1 [78]. Since a zero-range interaction (3) is used in the pp channel, the pairing strength V_0 is connected with a truncation in the quasiparticle space. The Borromean feature of ^{22}C is used to fix the pairing parameters as: $\rho_{\text{sat}} = 0.152 \text{ fm}^{-3}$, $V_0 = 355 \text{ MeV} \cdot \text{fm}^3$, and a cut-off energy $E_{\text{cut}}^{\text{q.p.}} = 60 \text{ MeV}$ in the quasiparticle space. These parameters result in $S_n = -28 \text{ keV}$ for ^{21}C and $S_{2n} = 0.43 \text{ MeV}$ for ^{22}C .

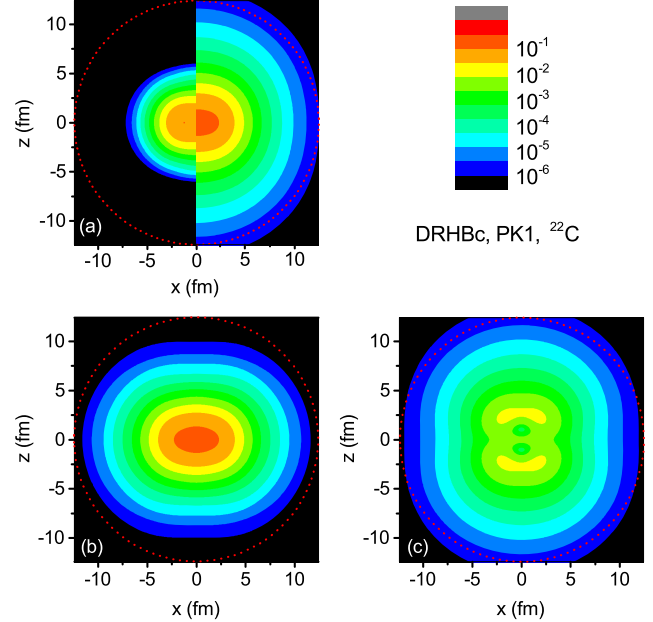


Fig. 1. (Color online) Density profiles of ^{22}C with the z axis as the symmetry axis. (a) The proton ($x < 0$) and neutron ($x > 0$) density profiles, (b) the density profile of the neutron core, and (c) the density profile of the neutron halo. In each plot, a dotted circle is drawn to guide the eye.

3. Results and discussions

In Fig. 1, we display the density profiles of ^{22}C . The density distribution of the protons and neutrons are shown in the left and right parts of Fig. 1(a), respectively. It is clearly seen that the neutrons extend spatially much farther than the protons, hinting a neutron halo in ^{22}C . The calculated matter radius $r_m = 3.25 \text{ fm}$ is significantly smaller than the experimental value $5.4 \pm 0.9 \text{ fm}$ given in 2010 [37] but close to the value $3.44 \pm 0.08 \text{ fm}$ obtained in 2016 [38] and $3.38 \pm 0.10 \text{ fm}$ extracted recently [39].

It should be mentioned that the empirical radius formula $r_m = 1.2A^{1/3} \text{ fm}$ gives 3.36 fm for $A = 22$ isobars [79]. This fact indicates that the halo in ^{22}C is not so pronounced if we adopt r_m values from Refs. [38,39] or from our calculations. Having in mind that the two-neutron separation energy S_{2n} is quite small ($\leq 0.5 \text{ MeV}$) as we have mentioned, such “small” r_m values are quite puzzling if one accepts the assumption that the valence neutrons in ^{22}C occupy mostly the $2s_{1/2}$ state. Next we address this issue by examining the halo configuration.

The augmented Lagrangian method [80] was implemented in the DRHBC model and deformation constraint calculations are carried out for ^{22}C . In Fig. 2, we show single neutron levels around the Fermi surface in the canonical basis. The ground state of ^{22}C locates at $\beta_2 = -0.27$, as indicated by the grey vertical line. There are several orbitals close to the Fermi level and the particle emission threshold: $1/2_3^+$ is weakly bound and $3/2_2^+$ and $1/2_4^+$ are in the continuum. These states contribute mostly to the halo and its deformation in ^{22}C as we will show later. From Fig. 2 one can find that $1/2_3^+$ becomes more deeply bound with β_2 increasing from the ground state and joins $1d_{5/2}$ with $\varepsilon_{\text{can}} \sim -3.6 \text{ MeV}$ at $\beta_2 = 0$. On the other hand, from the ground state to the spherical limit, $3/2_2^+$ and $1/2_4^+$ get closer in energy and finally merge as $1d_{3/2}$ which is around 1 MeV above the threshold. The single neutron levels in the canonical basis in the spherical limit and at the ground state are also shown in Fig. 3.

It is interesting to see in Figs. 2 and 3 that, in the spherical limit, the $2s_{1/2}$ state is lower than $1d_{5/2}$, i.e., these two states are

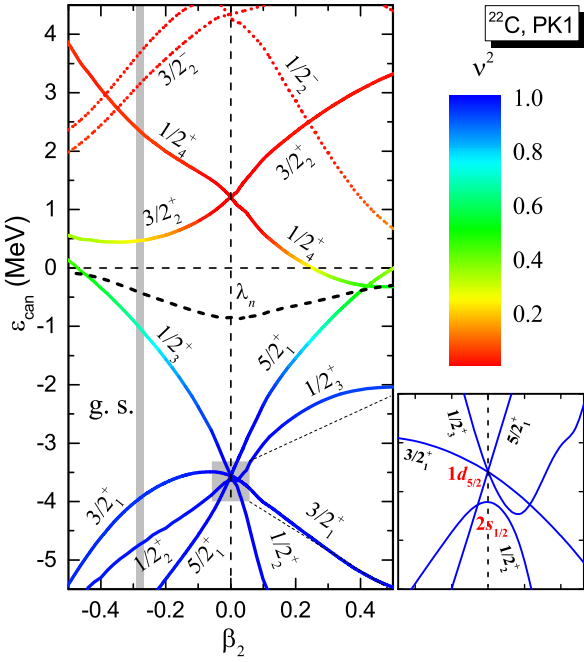


Fig. 2. (Color online) Single neutron orbitals around the Fermi level of ^{22}C in the canonical basis obtained from constraint calculations. We label each level with Ω_i^π where π is the parity, Ω is the projection of angular momentum on the symmetry axis, and i is used to order the level in each Ω^π -block. The Fermi level (λ_n) is displayed by the black dashed line. The occupation probability v^2 of each orbital is represented with different colors. The grey vertical line at $\beta_2 = -0.27$ corresponds to the ground state (g. s.) of ^{22}C . The shaded region with $-0.07 \leq \beta_2 \leq 0.07$ and $-3.8 \text{ MeV} \leq \epsilon_{\text{can}} \leq -3.4 \text{ MeV}$ is enlarged and shown on the right side.

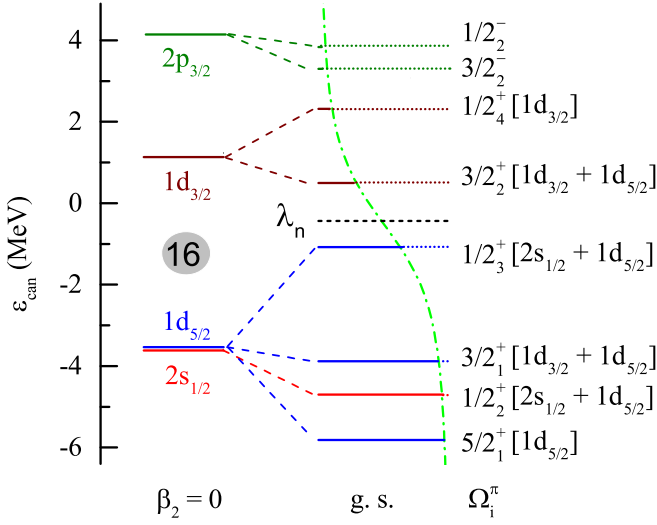


Fig. 3. (Color online) Single neutron orbitals around the Fermi level (λ_n) of ^{22}C in the canonical basis in the spherical limit and at the ground state (g. s.). For the case of the ground state, the length of the solid line is proportional to the occupation probability of each level calculated from the DRHbc model. The dash-dotted line corresponds to the occupation probability calculated from the BCS formula with an average pairing gap. Quantum numbers Ω_i^π and the main Woods-Saxon components are given for orbitals in the sd shell.

inverted compared with the conventional shell structure in stable nuclei. This inversion, together with the large spin-orbit splitting between the two d states, results in a noticeable shell gap at $N = 16$ when ^{22}C is constrained to be spherical. The inversion of $(2s_{1/2}, 1d_{5/2})$ has been predicted in $A/Z \sim 3$ nuclei [81] and the appearance of the $N = 14$ and $N = 16$ shell closures is closely

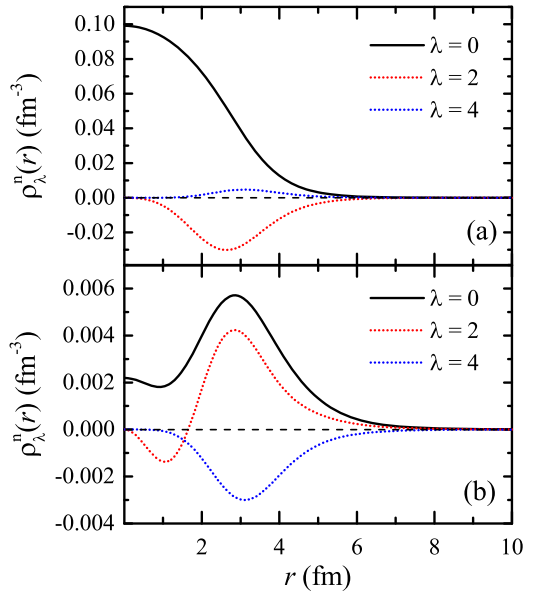


Fig. 4. Decomposition of the neutron density into spherical ($\lambda = 0$), quadrupole ($\lambda = 2$), and hexadecapole ($\lambda = 4$) components for (a) the core and (b) the halo of ^{22}C .

related to the competition of $2s_{1/2}$ and $1d_{5/2}$ [16,28,81–88]. In Ref. [56], it is shown that by decreasing the parameter t_0 in the Skyrme interaction SIII, the $2s_{1/2}$ orbital approaches $1d_{5/2}$ and finally can be lower than the latter in ^{22}C .

It has been well accepted that the inversion of $(2s_{1/2}, 1d_{5/2})$ results in the formation of the halo in ^{11}Li where the $2s_{1/2}$ orbital is close to $1p_{1/2}$ [5,89–91]. This inversion, however, plays an opposite role in ^{22}C : It hinders the halo formation when we stick to the spherical limit because the valence neutrons occupy a d -wave orbital. However, there are strong quadrupole correlations which drive ^{22}C to be well deformed with $\beta_2 = -0.27$. On the one hand, the deformation effects mix the sd orbitals, increase the neutron level densities around the Fermi surface, and destroy the $N = 16$ shell closure as is seen in Figs. 2 and 3. On the other hand, the mixture of the sd orbitals results in non-negligible $2s_{1/2}$ components in $1/2_3^+$ and $1/2_4^+$ which are either weakly bound or in the continuum. The total amplitude of the $2s_{1/2}$ component is about 0.25 in these two $1/2^+$ orbitals. Having in mind the degeneracy two, this means that about half of the valence neutrons is of the $2s_{1/2}$ nature. Therefore the neutron halo in ^{22}C is shrunk compared with what it would be if the halo configuration is dominated by $(2s_{1/2})^2$.

In Figs. 2 and 3, one can see that there is a large gap between $3/2_1^+$ and $1/2_3^+$. The orbital $3/2_1^+$ and those below it are deeply bound and contribute to the “core”. The orbital $1/2_3^+$ and those above it, the sum of occupation probabilities of which being 1.03, are weakly bound or in the continuum and form the “halo”. In such a way we can decompose the neutron density into two parts. The density profiles of the neutron core and halo are presented in Figs. 1(b) and (c), respectively. It is clearly seen that the core of ^{22}C is oblate and the halo is prolate. This provides one more example of deformed nuclei with a shape decoupling besides ^{42}Mg and ^{44}Mg , both with a prolate core but an oblate halo [18,19].

In Fig. 4 the densities of the core and the halo of ^{22}C are decomposed into spherical ($\lambda = 0$), quadrupole ($\lambda = 2$), and hexadecapole ($\lambda = 4$) components [cf. Eq. (5)]. In Fig. 4(a), it can be found that the quadrupole component of the core is always negative, which corresponds to the oblate shape of ^{22}C . However, as seen in Fig. 4(b), although it is negative when $r < 1.6$ fm, the

